Hindawi Publishing Corporation
International Journal of Photoenergy
Volume 2013, Article ID 925280, 9 pages
http://dx.doi.org/10.1155/2013/925280

Research Article

Effect of Temperature and Humidity on the Degradation Rate of Multicrystalline Silicon Photovoltaic Module

N. C. Park,[1] W. W. Oh,[2] and D. H. Kim[2]

[1] *Components & Materials Physics Research Center, Korea Electronic Technology Institute, No. 68 Yaptap-dong, Bundang-gu, Seongnam-si, Gyeonggi-do 463-816, Republic of Korea*
[2] *Department of Materials Science and Engineering, Korea University, Anam-dong, Seongbuk-gu, Seoul 136-701, Republic of Korea*

Correspondence should be addressed to N. C. Park; ncpark@keti.re.kr and D. H. Kim; solar@korea.ac.kr

Received 2 October 2013; Accepted 14 November 2013

Academic Editor: Dionissios Mantzavinos

In a PV module, the relative humidity (rh) of a front encapsulant is different from that of a backside encapsulant (rh_{back}). In this study, the effective humidity (rh_{eff}) in a PV module was investigated to study the effects of moisture variation on the degradation rate (R_D). rh_{eff} represents uniform humidity in a PV module when it is exposed to certain damp heat conditions. Five types of accelerated tests were conducted to derive the relation between rh_{eff} and rh_{back}. rh_{eff} showed a linear relationship with rh_{back} at constant temperature. Two types of models, namely, Eyring and Peck models, were used for predicting the R_D of PV modules, and their results were compared. The R_D of PV modules was thermally activated at 0.49 eV. Furthermore, the temperature and rh_{eff} history of PV modules over one year were determined at two locations: Miami (FL, USA) and Phoenix (AZ, USA). The accumulated R_D values based on the temperature and rh_{eff} of the modules were calculated by summing the hourly degradation amounts over the time history.

1. Introduction

Moisture can diffuse into photovoltaic (PV) modules through their breathable back sheets or their ethylene vinyl acetate (EVA) sheets [1]. When in service in hot and humid climates, PV modules experience changes in the moisture content, the overall history of which is correlated with the degradation of the module performance [1]. If moisture begins to penetrate the polymer and reaches the solar cell, it can weaken the interfacial adhesive bonds, resulting in delamination [2] and increased numbers of ingress paths, loss of passivation [3], and corrosion of solder joints [4, 5]. Of these possibilities, the occurrence of corrosion has one of the highest frequencies in outdoor-exposed PV modules [6]. Significant losses in PV module performance are caused by the corrosion of the cell, that is, the SiNx antireflection coating, or the corrosion of metallic materials, that is, solder bonds and Ag fingers [7, 8]. Corrosion is defined as the destructive chemical or electrochemical reaction of a metal with its environment. The moisture from the environment may lead to electrochemical reactions that can result in corrosion. For the electrochemical reaction of metals with their environment, an aqueous, ion-conduction enabling environment is necessary; moreover, at high temperatures, gas-metal reactions are possible [9]. The International Electrotechnical Commission (IEC) 61215 test defines a damp heat (DH) test in 10.13. The DH test is conducted for determining the effect of long-term penetration of humidity on materials. Therefore, many researchers have studied the reliability of PV modules on the basis of IEC 61215. Laronde et al. [10] have employed DH testing to study the degradation of PV modules subjected to corrosion. Peike et al. [11] have reported that grid corrosion or reduced conductivity between the emitter and grid is the most likely cause of DH-induced degradation. They have also shown that high temperatures accelerate water vapor permeation into the module and the subsequent degradation reactions. Furthermore, it has been reported that loss of adhesion strength is exacerbated by

exposure to high humidity environments [2] and facilitates the delamination of EVA from the cell [3], which results in grid corrosion [12]. Therefore, in order to understand the effect of grid corrosion on the degradation of PV modules, one needs to comprehend how the surrounding environment affects the module temperature (T_m) and moisture content of the module. Kempe [1] has suggested that analytical equations can be used to determine timescales for moisture ingress with breathable back sheets. Koehl et al. [13] have showed that the maximum moisture concentration in front of a cell was not reached after 1,000 h under DH conditions at 85°C and 85% rh because of the long path to the back sheet. They have also documented that the humidity in front of the cell is not directly influenced by ambient fluctuations in actual weather conditions.

As mentioned above, PV modules are degraded by ambient temperature and humidity; moreover, these factors can accelerate the degradation. This degradation is mainly caused by corrosion [4, 5, 7, 8, 10, 11]. It can be assumed that the temperature of a PV module is uniform; however, moisture concentration in a PV module is not uniform. Therefore, it is difficult to predict moisture-induced degradation.

Therefore, in this study, effective humidity (rh_{eff}) in a PV module was investigated to study the effect of moisture variation in a PV module. rh_{eff} represents uniform humidity in a PV module when it is exposed to certain DH conditions. This paper documents the relation of rh_{eff} with ambient temperature and humidity. Moreover, the resultant module degradation rate (R_D) for various rh_{eff} values is also reported in this paper. These data allow the prediction of real-world thermal- and moisture-induced R_D values of PV modules and enable the computation of acceleration factor (AF) for the DH test.

2. Experiments

Six-inch multicrystalline Si (m-Si) solar cells were used in this study. The typical characteristics of the cells at a light intensity of 1 sun were approximately as follows: open-circuit voltage (V_{oc}), 0.60 V; short-circuit current density (J_{sc}), 33.9 mA/cm^2; fill factor (FF), 0.72; and conversion efficiency, 16.8%.

A copper ribbon wire, which was plated with 62Sn36Pb2Ag solder, was used for cell interconnection. The dimensions of the ribbon wire were 0.15 mm × 1.5 mm. The samples were divided into two groups on the basis of lamination conditions. Type 1 was arranged with EVA, cell, and EVA. Type 2 was laminated with low-iron glass of area 180 mm × 180 mm and thickness 3.2 mm, an EVA of thickness 0.35 mm, a cell, an EVA, and a TPT back sheet of thickness 0.35 mm, as shown in Figures 1(a), 1(b), and 1(c). The solar cells were laminated with EVA by heating them up to 150°C for 12 min. After encapsulation, the samples were divided into five groups and exposed to accelerated stresses, as shown in Table 1. Five kinds of test conditions were selected: 85°C, 85% rh (8585), 65°C, 85% rh (6585), and 45°C, 85% rh (4585) for temperature acceleration and 65°C, 75% rh (6575), and 65°C, 65% rh (6565) for humidity acceleration. A total of five cases, each with ten samples, were tested. DH conditions were obtained in an environmental chamber (Hygros340C, ACS Co., Massa Martaba, Italy).

Table 1: Test conditions for accelerated tests.

Number	Temperature (°C)	Relative humidity (%)	Sample size (EA)
1	85	85	10
2	65	85	10
3	45	85	10
4	65	75	10
5	65	65	10

The electrical performance of each sample was measured every 200 h using a solar simulation system (K202 Lab200, Mac Science, Seoul, South Korea). The standard test conditions were (a) irradiance: 1000 W/m^2, (b) cell temperature: 25°C, and (c) spectral distribution of irradiance: AM 1.5 G (IEC 60904-3).

Accelerated tests (ATs) were conducted for 4,500 h for 8585, 6585, and 4585 and for 3,200 h for 6575 and 6565. The maximum power of all samples decreased by over 5% after the ATs. Using the results, the average R_D for each condition was calculated.

3. R_D Prediction Models and Effective Humidity

R_D data can be postulated with an empirical kinetic model by assuming that the rate of degradation is proportional to the concentration of water in PV modules, and that the rate constant has Arrhenius temperature dependence.

Escobar and Meeker [14] has proposed two degradation models: variations of Eyring and Peck models, which are used for operating conditions when temperature and humidity are the accelerated stresses in a test. The degradation rate based on the Eyring model ($R_{D,\text{Eyring}}$) is given by

$$R_{D,\text{Eyring}} = A \exp\left(\frac{-E_a}{kT} - \frac{b}{\text{rh}}\right), \quad (1)$$

where E_a is the thermal activation energy of the degradation process (eV), k is the Boltzmann constant (8.62×10^{-5} eV/K), T is the temperature (°K), and rh is the relative humidity (%). A and b are two constants dependent on the failure mode. R_D (%/h) is the inverse of the mean time to failure (MTTF) at a given condition. In order to obtain R_D, we determined the time to 5% reduction in the initial maximum power ($P_{\max}$) at all samples. The life distributions were determined with ALTA 7 software. Using the results, the MTTF was calculated.

The other degradation model based on the Peck model ($R_{D,\text{Peck}}$) is expressed as follows:

$$R_{D,\text{Peck}} = B \exp\left(\frac{-E_a}{kT}\right) \cdot (\text{rh})^n, \quad (2)$$

where B and n are two constants dependent on the failure mode.

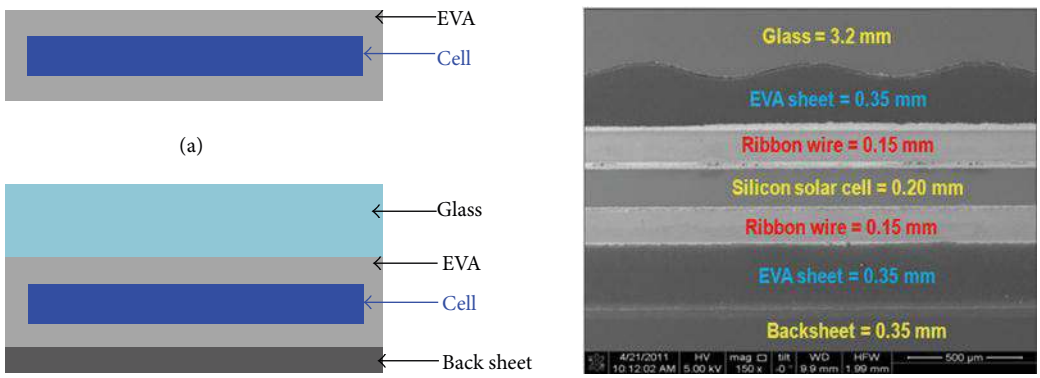

Figure 1: Test samples for DH tests: (a) PV module with EVA/cell/EVA structure (Type 1), (b) PV module with glass/EVA/cell/EVA/back sheet structure (Type 2).

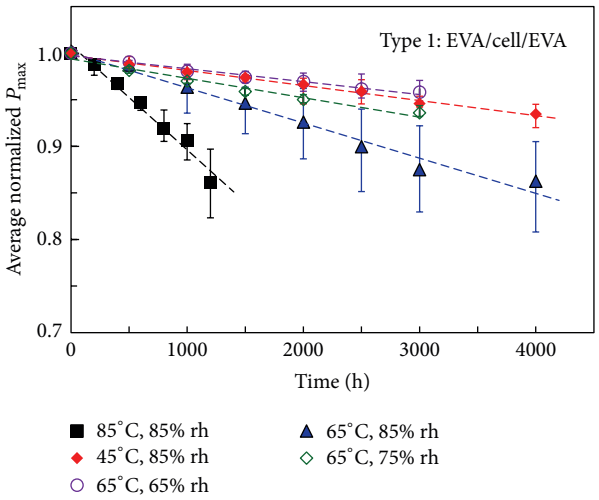

Figure 2: Average normalized P_{max} of Type 1 as a function of time.

In order to obtain A, E_a in (1) and B, n in (2), the equations can be represented on a logarithmic scale by a straight line, using the following equations:

$$\ln\left(R_{D,\text{Eyring}}\right) = \ln\left(A\right) - \left(\frac{E_a}{kT}\right) - \left(\frac{b}{\text{rh}}\right),$$
$$\ln\left(R_{D,\text{Peck}}\right) = \ln\left(B\right) - \left(\frac{E_a}{kT}\right) + n\ln\left(\text{rh}\right). \quad (3)$$

A plot of the left-hand side of (3) versus $1/T$ (°K) gives an Arrhenius plot with a slope E_a/k and an intercept $\ln(k_0)$.

$\ln(R_D)$ versus $1/T$ (°K) gives an Arrhenius plot with a slope E_a/k and intercepts $\ln(A)$ and $\ln(B)$.

The rh in PV modules depends on their ambient climate, material (encapsulant, back sheet) properties, and the operation conditions. If all information is available, moisture concentration in the backside encapsulant can be calculated using the diffusion model [1]. However, the moisture concentration in the front encapsulant is different from that at the back of the cell because of the long path from the back sheet [13]. In a 85°C, 85% rh test, the maximum moisture content in the backside encapsulant was reached quickly; however, the maximum moisture content of the front encapsulant was not reached even after 1,000 h of exposure time [13]. Therefore, rh_{eff} of a PV module was considered to determine the uniform moisture content in the module.

In order to derive the effect of uniform humidity in a PV module on its degradation, PV modules with a EVA/cell/EVA structure (Type 1) were used as shown in Figure 1(a). This is because the cell and EVA layer structure allow water vapor to permeate the surface of the cell within minutes during the DH test [15].

In case of Type 1, it can be assumed that the rh in the PV module is uniform. If E_a and constants (A, B, etc.) are determined, the degradation rate of Type 1 ($R_{D,\text{Type1}}$) can be predicted with

$$R_{D,\text{Type1,Eyring}} = A_1 \exp\left(\frac{-E_{a,\text{Type1}}}{kT_1} - \frac{b_1}{\text{rh}_1}\right),$$
$$R_{D,\text{Type1,Peck}} = B_1 \exp\left(\frac{-E_{a,\text{Type1}}}{kT_1}\right) \cdot \left(\text{rh}_1\right)^{n_1}. \quad (4)$$

However, in case of glass/EVA/cell/EVA/back sheet structure (Type 2), rh is not uniform in the PV module. Therefore, it is difficult to fix the rh in the PV module. If $R_{D,\text{Type2}}$ is known, $R_{D,\text{Type2}}$ is expressed with the right-hand side of (4), and rh_{eff} is as follows:

$$R_{D,\text{Type2}} = A_1 \exp\left(\frac{-E_{a,\text{Type1}}}{kT_1} - \frac{b_1}{\text{rh}_{\text{eff,Eyring}}}\right),$$
$$R_{D,\text{Type2}} = B_1 \exp\left(\frac{-E_{a,\text{Type1}}}{kT_1}\right) \cdot \left(\text{rh}_{\text{eff,Peck}}\right)^{n_1}, \quad (5)$$

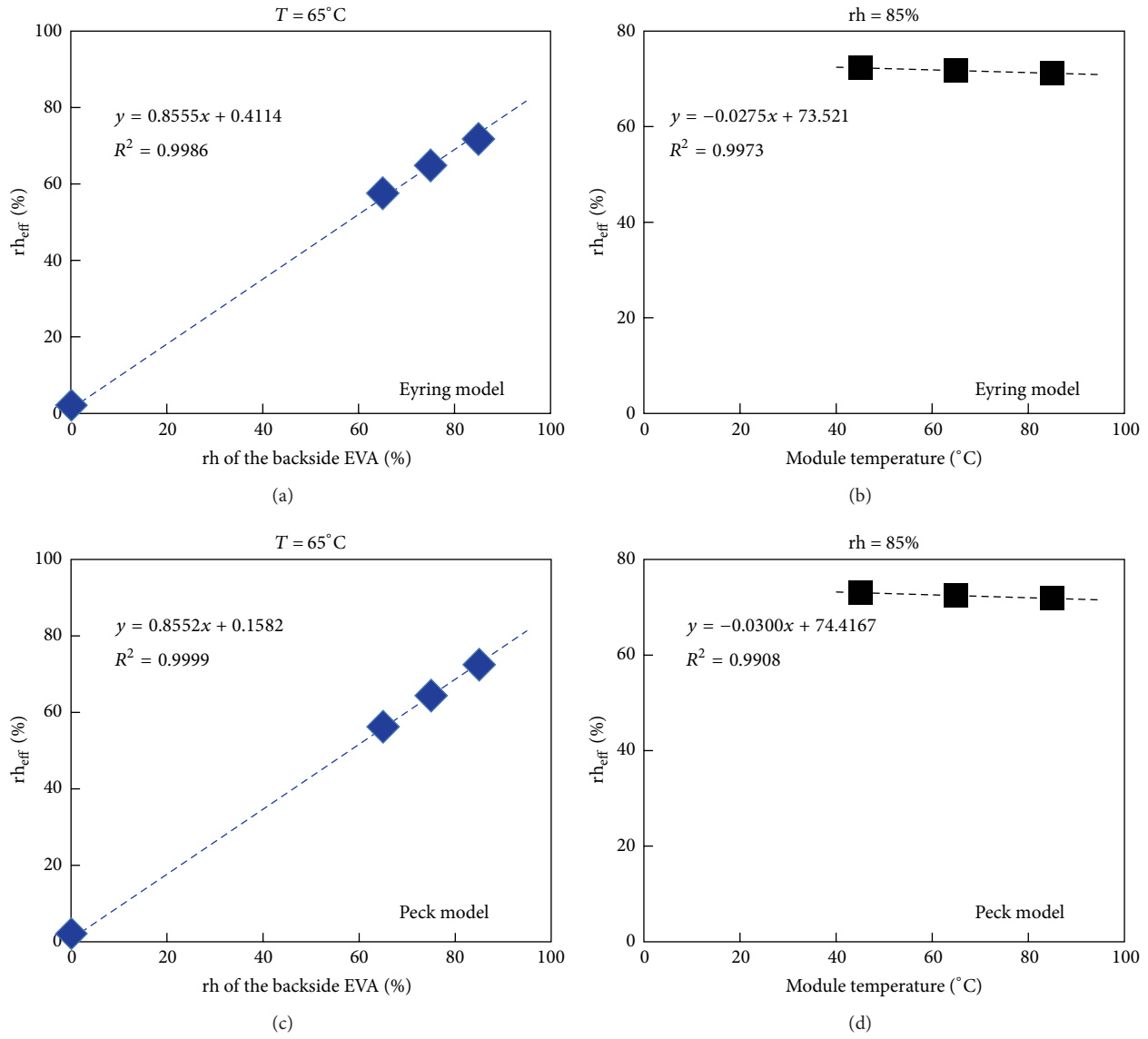

FIGURE 3: rh_{eff} versus rh for the backside EVA and rh_{eff} versus module temperature are plotted for two R_D prediction models: (a) rh_{eff} versus rh for the backside EVA at constant temperature for Eyring model, (b) rh_{eff} versus module temperature at constant humidity for Eyring model, (c) rh_{eff} versus rh for the backside EVA at constant temperature for Peck model, (d) rh_{eff} versus module temperature at constant humidity for Peck model.

where $E_{a,\text{Type1}}$ and other parameters (A_1, b_1, B_1, and n_1) can be determined by ATs as shown in Table 1. Using (5), rh_{eff} is rearranged as follows:

$$rh_{\text{eff,Eyring}} = \frac{-b_1}{\ln\left(R_{D,\text{Type2}}\right) - \ln A_1 + \left(E_{a,\text{Type1}}/kT_1\right)}, \quad (6)$$

$$rh_{\text{eff,Peck}} = \left(\frac{R_{D,\text{Type2}}}{B_1 \exp(-E_{a,\text{Type1}}/kT_1)}\right)^{1/n_1}. \quad (7)$$

4. Results

4.1. Results of Accelerated Tests. The changes in average normalized P_{max} of the modules in Type 1 as a function of time are plotted in Figure 2. The figure shows that P_{max} decreases linearly over time. The results correspond well with those found in earlier studies [6, 16]. Several authors [17, 18] argue that the limited experimental evidence available is not enough to take the linear R_D for granted and suggest that an exponential degradation rate could be a more suitable trend as is the case in some optoelectronic devices. However, it should be noted that both trends exhibit very similar evolution during the first 10–15 years; if similar initial annual degradation rates are assumed, then the linear degradation rate is a more pessimistic estimate [19].

In order to keep the discussions simple, we will not consider the exponential degradation rate here.

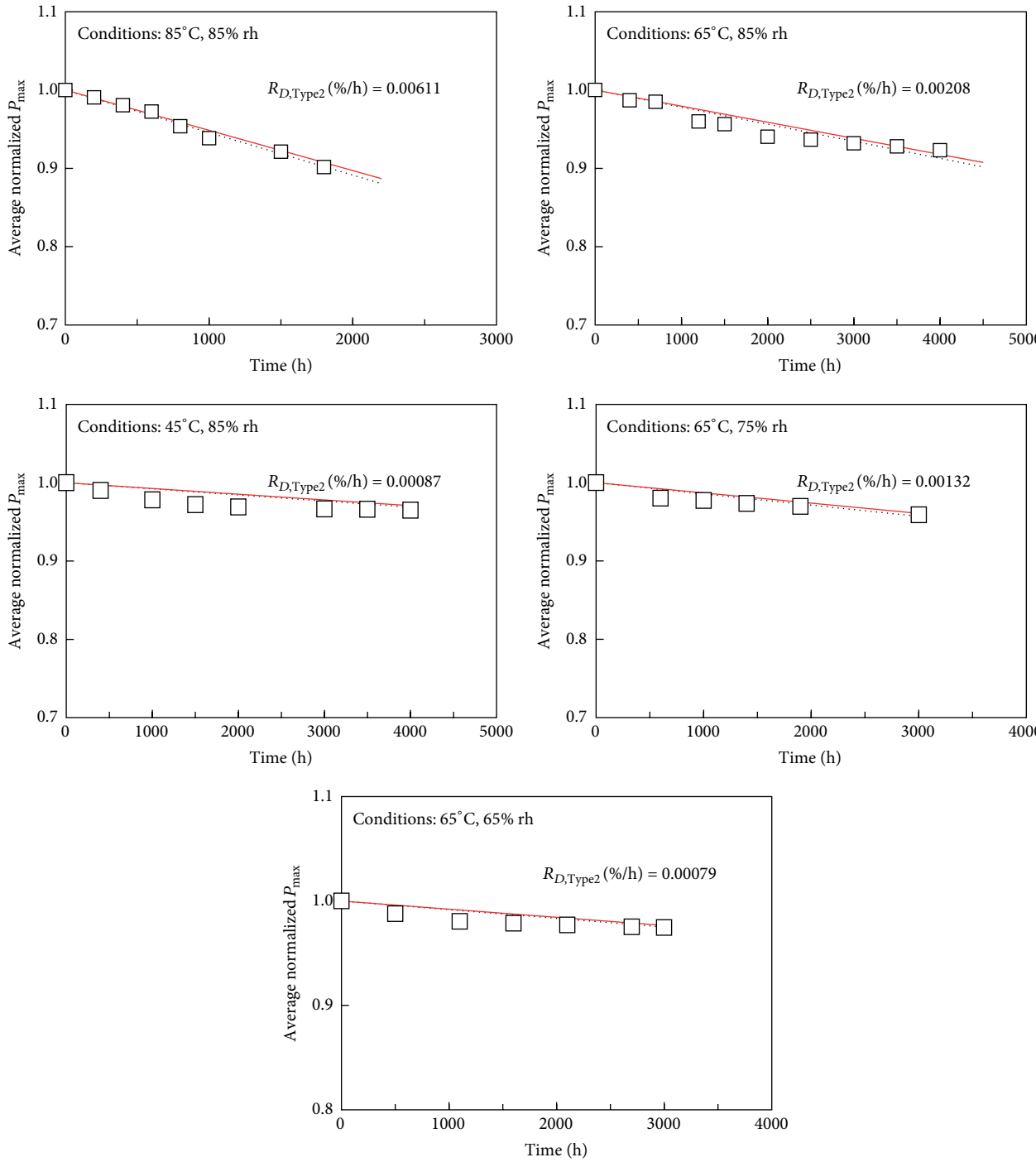

Figure 4: Average normalized P_{max} of Type 2 as a function of time. □ shows the measurement data, dotted line (black) shows the predicted degradation rate obtained using (1), and straight line (red) shows the predicted degradation rate obtained using (2).

Using AT results of Type 1 samples, the R_D was determined for each set of conditions.

E_a is obtained by fitting the R_D data in (1) and (2) for three values of temperature. $E_{a,Type1}$ and other constants were calculated as summarized in Table 2.

$R_{D,Type2}$ of the modules was also determined for each set of conditions. The R_D values (%/h) of 8585, 6585, 4585, 6575, and 6565 were 0.00611, 0.00208, 0.00087, 0.00132, and 0.00079, respectively.

In order to derive the relationship between rh_{eff} and rh in the backside encapsulant, $R_{D,Type2}$ in (4) was replaced with R_D values. Figure 3 shows a plot of rh_{eff} versus rh in the backside encapsulant at a constant temperature and constant humidity. In both models, rh_{eff} versus rh has a linear

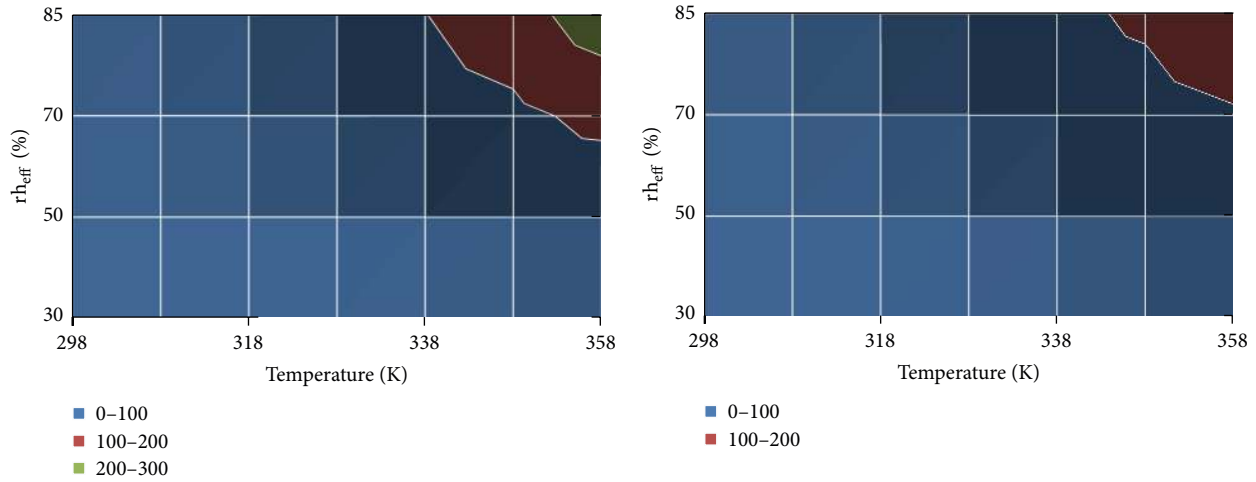

Figure 5: AF Contours of module temperature and rh_{eff} for two R_D prediction models: (a) Eyring model, (b) Peck model.

Table 2: Activation energy and constants of Type 1 samples for Eyring and Peck models.

Model	E_a	A_1	b_1	B_1	n_1
Eyring	0.49	2.40×10^6	281.86	—	—
Peck		—	—	0.0037	3.82

relation at a constant temperature, and rh_{eff} decreases linearly with temperature at constant humidity (inset in Figure 3). Therefore, rh_{eff} is expressed as follows:

$$rh_{eff,Eyring} = [(73.521 - 0.0275 \cdot T)] \cdot \frac{0.8555 rh_{back} + 0.4114}{71.2}, \quad (8)$$

$$rh_{eff,Peck} = [(74.417 - 0.0300 \cdot T)] \cdot \frac{0.8552 rh_{back} + 0.1584}{71.9}. \quad (9)$$

Using rh_{eff} values at AT conditions, predicted R_Ds$_{,Type2}$ of (5) are plotted as a function of time in Figure 4. It shows that the predicted $R_{D,Type2}$ is almost identical to the measured data.

4.2. Acceleration Factor. AF is defined as the ratio between the R_D at a given temperature, rh_{eff} and R_D at a reference temperature, and rh_{eff} (in our case 25°C, 50% rh) [20]. AF is expressed as

$$AF_{Eyring} = \exp\left[-\frac{E_{a,Type1}}{k}\left(\frac{1}{T_0} - \frac{1}{T}\right) + b_1\left(\frac{1}{rh_0} - \frac{1}{rh_{eff}}\right)\right],$$

$$AF_{Peck} = \exp\left[-\frac{E_{a,Type1}}{k}\left(\frac{1}{T_0} - \frac{1}{T}\right)\right]\left(\frac{rh_0}{rh_{eff}}\right)^{n_1}, \quad (10)$$

where T_0 and rh_0 are the reference temperature and reference humidity, respectively.

Figure 5 shows the AF contours on plots of rh_{eff} versus module-temperature data. Estimated AFs for the 8585 condition versus 25°C, 50% rh range from 190× to 250× for the Peck and Eyring models, respectively. However, in real-world operation, a constant temperature and rh are not realistic. To project field R_D at a specific location, it was characterized by the annual module temperature and rh of the backside encapsulant.

5. R_D in Two Benchmark Climates

Two benchmark climates (BMCs) were selected to quantify the stress: Miami (FL, USA) and Phoenix (AZ, USA). The module-temperature history exposed to the two BMCs was derived from meteorological data [21]. Meteorological data for Miami, FL, for 2005 and Phoenix, AZ, for 2002 were obtained from the National Climatic Data Center.

The rh of the backside encapsulant was calculated using the model of moisture ingress [1]. We determined the activation energy for encapsulant solubility in a previous research [22]. E_a for maximum water vapor transmission rate ($WVTR_{max}$) of back sheets was evaluated. The transient WVTR was measured using a WVTR instrument (Permatran-W$^{3/33}$, Mocon, Minneapolis, MN, USA) at 25°C, 37.8°C, and 50°C. Assuming an Arrhenius equation between $WVTR_{max}$ and temperature, $WVTR_{max}$ can be described by

$$WVTR_{max} = A \exp\left(\frac{-E_w}{kT}\right). \quad (11)$$

Parameters A and E_w were obtained from a curve fit of a plot of of $\ln(WVTR_{max})$ versus $1/kT$. The A and E_w values are 2.703×10^6 g/m^2/day and 0.367 eV, respectively.

The accumulated R_D based on the module temperature and rh_{eff} can be calculated by summing the hourly degradation amounts over the time history, as given by

$$\sum R_{D,Type2} \cdot t = \left[A_1 \exp\left(\frac{-E_{a,Type1}}{kT_1} - \frac{b_1}{rh_{eff,Eyring}}\right)\right] \cdot t,$$

$$\sum R_{D,Type2} \cdot t = \left[B_1 \exp\left(\frac{-E_{a,Type1}}{kT_1}\right) \cdot (rh_{eff,Peck})^{n_1}\right] \cdot t. \quad (12)$$

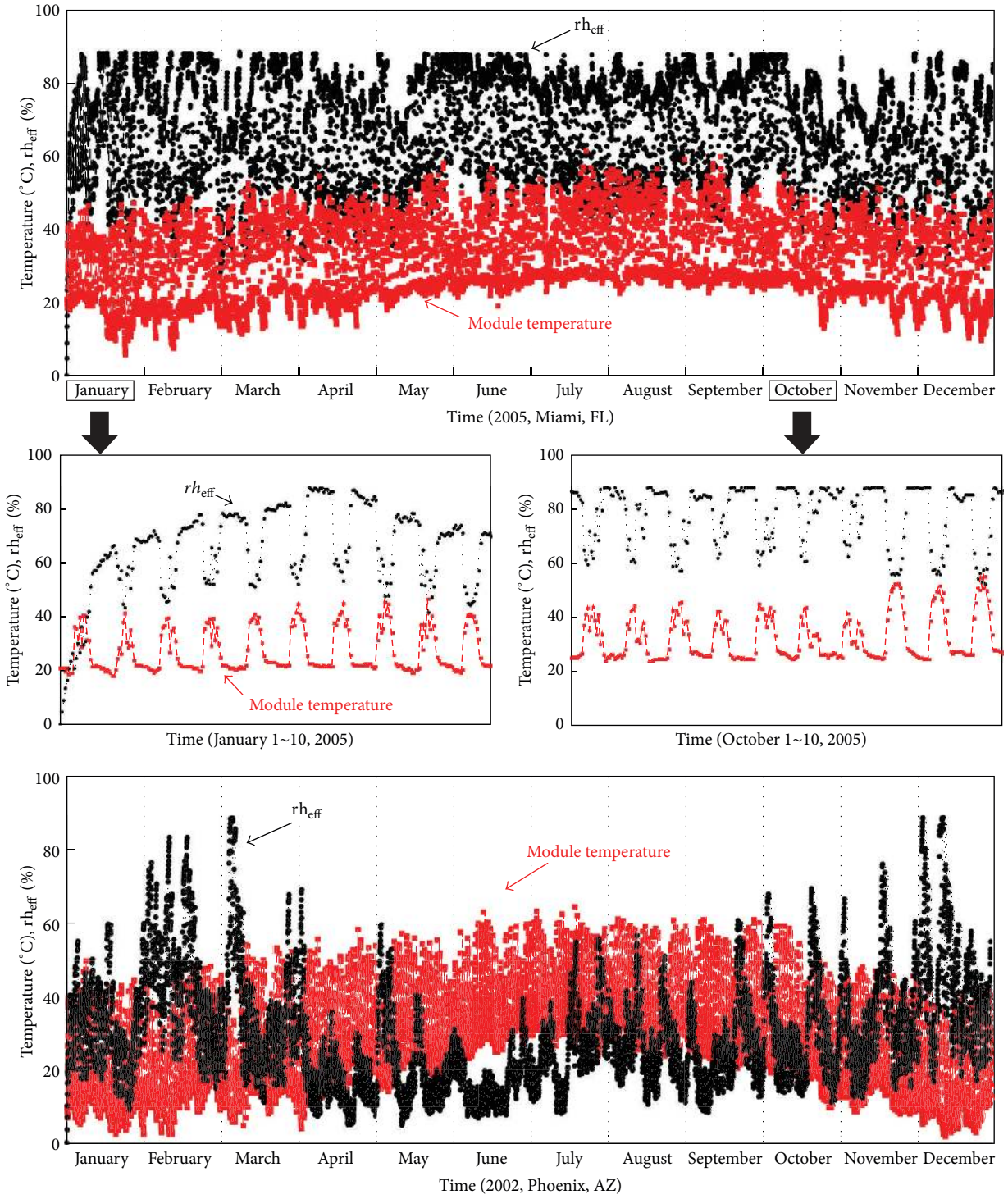

FIGURE 6: Module temperature and rh_{eff} over one year in 2 benchmark climates. rh_{eff} is determined with (8) for Eyring model.

Thermal and $rh_{eff,Eyring}$ history of a PV module over one year were calculated at two BMCs as shown in Figure 6. Compared with Miami, the module temperature at Phoenix is shifted more than 10°C higher and the rh_{eff} has a relatively low distribution.

Accumulated R_D in the two BMCs is calculated using (12), which are based on the module temperature and rh_{eff} of Figure 6.

The normalized $R_{D,Eyring}$ and $R_{D,Peck}$ of the PV module exposed to two BMCs are plotted over one year in Figure 7(a). The accumulated $R_{D,Peck}$ was 3.0% greater than $R_{D,Eyring}$ in Miami. The conditions of 8585 are normally used for DH tests as IEC 61215. Therefore, the accumulated R_D exposed to 8585 was evaluated and compared to the accumulated R_D in the Miami. The accumulated $R_{D,Eyring}$ and $R_{D,Peck}$ for exposure to 8585 were about 23.7 and 23.1 times greater than those in

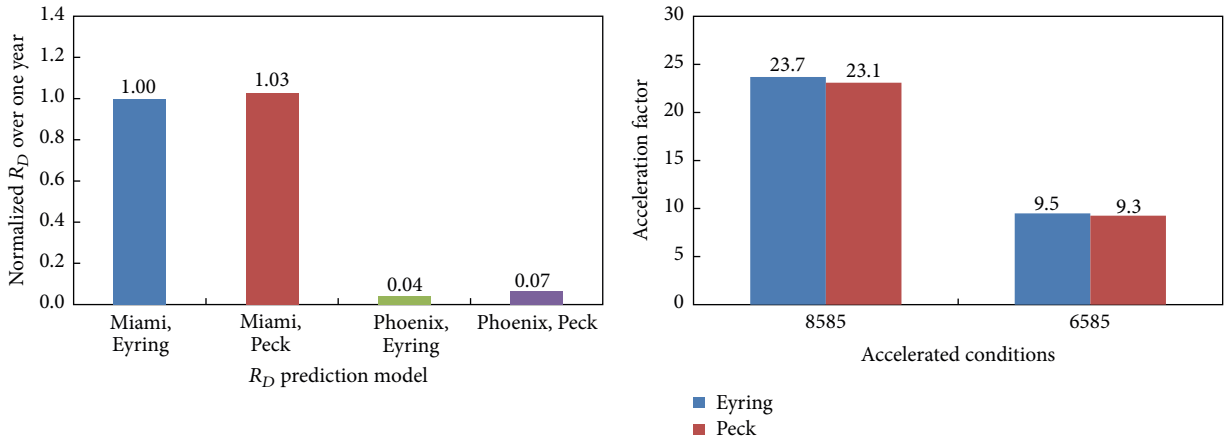

FIGURE 7: Normalized R_D exposure to actual weather conditions for 1 year and AF of accelerated conditions: (a) normalized $R_{D,\text{Eyring}}$ and $R_{D,\text{Peck}}$ for an initially dry module after exposure to two BMCs, (b) AF exposure to 85°C, 85% rh and 65°C, 85% rh is compared to that at Miami (FL, 2005).

Miami, as shown in Figure 7(b). Koehl et al. [13] have reported that AF of 8585 is about 23 for a tropical site (Serpong, Indonesia), 40 for an arid site (Sede Boqer, Israel), and 106 for an alpine site (Zugspitze, Germany) for a degradation process with an activation energy of 0.416 eV.

In case of 6585, the R_D values according to Eyring and Peck models are 9.5 and 9.3 times greater than those in Miami. Therefore, it can be supposed that the Peck model is a slightly conservative estimation for R_D prediction.

6. Conclusions

The objectives of this study were to investigate the relation of ambient temperature and humidity with the rh_{eff} of a PV module and to use the rh_{eff} values to predict the R_D values under actual weather conditions.

The degradation of PV modules is accelerated by temperature and humidity [1, 4, 5, 10, 11]. It can be assumed that the temperature in a PV module is uniform. However, the moisture concentration is not uniform [13]. Therefore, we used a Type 1 module with a EVA/cell/EVA structure for uniform humidity in the module.

Two types of models, namely, Eyring and Peck models, were used for R_D prediction, and their results were compared with each other. Five types of ATs were conducted to determine E_a and humidity dependence. The R_Ds of PV modules were thermally activated at 0.49 eV.

The moisture content in a PV module is dependent on material properties such as back sheets and EVA. Therefore, we determined the relation between the rh of the backside encapsulant and rh_{eff}. rh of the backside encapsulant was calculated using the moisture ingress model. Thermal and rh_{eff} history of a PV module over one year were calculated in two BMCs. For exposure to 8585, the accumulated $R_{D,\text{Eyring}}$ and $R_{D,\text{Peck}}$ values at Phoenix were, respectively, about 23.7 and 23.1 times greater than those at Miami.

Abbreviation:

AF: Acceleration factor
AT: Accelerated tests
BMC: Benchmark climate
DH: Damp heat
EVA: Ethylene vinyl acetate
FF: Fill factor
IEC: International Electrotechnical Commission
J_{sc}: Short-circuit current density
MTTF: Mean time to failure
PV: Photovoltaic
R_D: Degradation rate
$R_{D,\text{Eyring}}$: Degradation rate based on the Eyring model
$R_{D,\text{Peck}}$: Degradation rate based on the Peck model
rh: Relative humidity
rh_{back}: Relative humidity of a backside encapsulant
rh_{eff}: Effective humidity
T_m: Module temperature
V_{oc}: Open-circuit voltage.

Acknowledgments

This work was supported by the New and Renewable Energy of the Korea Institute of Energy Technology Evaluation and Planning (KETEP) Grant funded by the Ministry of Trade, Industry and Energy (MOTIE) (no. 2012T100100605). Furthermore, this work was supported by the Human Resources Development of the Korea Institute of Energy Technology Evaluation and Planning (KETEP) Grant funded by the Korea Governments Ministry of Knowledge Economy (no. 20104010100640).

References

[1] M. D. Kempe, "Modeling of rates of moisture ingress into photovoltaic modules," *Solar Energy Materials and Solar Cells*, vol. 90, no. 16, pp. 2720–2738, 2006.

[2] K. Morita, T. Inoue, H. Kato, I. Tsuda, and Y. Hishikawa, "Degradation factor analysis of cRYSTALLINE-Si PV modules through long-term field exposure TEST," in *Proceddings of the 3rd World Conference on Photovoltaic Energy Conversion*, pp. 1948–1951, May 2003.

[3] E. E. van Dyk, J. B. Chamel, and A. R. Gxasheka, "Investigation of delamination in an edge-defined film-fed growth photovoltaic module," *Solar Energy Materials and Solar Cells*, vol. 88, no. 4, pp. 403–411, 2005.

[4] N. G. Dhere and N. R. Raravikar, "Adhesional shear strength and surface analysis of a PV module deployed in harsh coastal climate," *Solar Energy Materials and Solar Cells*, vol. 67, no. 1–4, pp. 363–367, 2001.

[5] X. Han, Y. Wang, L. Zhu, H. Xiang, and H. Zhang, "Mechanism study of the electrical performance change of silicon concentrator solar cells immersed in de-ionized water," *Energy Conversion and Management*, vol. 53, no. 1, pp. 1–10, 2012.

[6] D. Polverini, M. Field, E. Dunlop, and W. Zaaiman, "Polycrystalline silicon PV modules performance and degradation over 20 years," *Progress in Photovoltaics: Research and Applications*, vol. 21, no. 5, pp. 1004–1015, 2013.

[7] M. Köntges, V. Jung, and U. Eitner, "Requirements on metallization schemes on solar cells with focus on photovoltaic modules," in *Proceedings of the 2nd Workshop on Metallization of Crystalline Silicon Solar Cells*, 2010.

[8] C. Dechthummarong, B. Wiengmoon, D. Chenvidhya, C. Jivacate, and K. Kirtikara, "Physical deterioration of encapsulation and electrical insulation properties of PV modules after long-term operation in Thailand," *Solar Energy Materials and Solar Cells*, vol. 94, no. 9, pp. 1437–1440, 2010.

[9] E. E. Stansbury and R. A. Buchanan, *Fundamentals of Electrochemical Corrosion*, ASM International, 2000.

[10] R. Laronde, A. Charki, and D. Bigaud, "Lifetime estimation of a photovoltaic module subjected to corrosion due to damp heat testing," *Journal of Solar Energy Engineering*, vol. 135, no. 2, Article ID 021010, 8 pages, 2013.

[11] C. Peike, S. Hoffmann, P. Hülsmann et al., "Origin of damp-heat induced cell degradation," *Solar Energy Materials and Solar Cells*, vol. 116, pp. 49–54, 2013.

[12] M. A. Quintana, D. L. King, T. J. McMahon, and C. R. Osterwald, "Commonly observed degradation in field-aged photovoltaic modules," in *Proceedings of the 29th IEEE Photovoltaic Specialists Conference*, pp. 1436–1439, May 2002.

[13] M. Koehl, M. Heck, and S. Wiesmeier, "Modelling of conditions for accelerated lifetime testing of humidity impact on PV-modules based on monitoring of climatic data," *Solar Energy Materials and Solar Cells*, vol. 99, pp. 282–291, 2012.

[14] L. A. Escobar and W. Q. Meeker, "A review of accelerated test models," *Statistical Science*, vol. 21, no. 4, pp. 552–577, 2006.

[15] P. Hülsmann, K. A. Weiß, and M. Köhl, "Temperature–dependent water vapour and oxygen permeation through different polymeric materials used in photovoltaic–modules," *Progress in Photovoltaics: Research and Applications*, 2012.

[16] M. A. Green, "Silicon photovoltaic modules: a brief history of the first 50 years," *Progress in Photovoltaics: Research and Applications*, vol. 13, no. 5, pp. 447–455, 2005.

[17] J. Xie and M. Pecht, "Reliability prediction modeling of semiconductor light emitting device," *IEEE Transactions on Device and Materials Reliability*, vol. 3, no. 4, pp. 218–222, 2003.

[18] S. L. Chuang, A. Ishibashi, S. Kijima, N. Nakayama, M. Ukita, and S. Taniguchi, "Kinetic model for degradation of light-emitting diodes," *IEEE Journal of Quantum Electronics*, vol. 33, no. 6, pp. 970–979, 1997.

[19] M. Vázquez and I. Rey-Stolle, "Photovoltaic module reliability model based on field degradation studies," *Progress in Photovoltaics: Research and Applications*, vol. 16, no. 5, pp. 419–433, 2008.

[20] M. Ohring, *Reliability and Failure of Electronic Materials and Devices*, Academic Press, New York, NY, USA, 1998.

[21] D. L. King, W. E. Boyson, and J. A. Kratochvill, *Photovoltaic Array Performance Model*, United States Department of Energy, Washington, DC, USA, 2004.

[22] N. Park, C. Han, and D. Kim, "Effect of moisture condensation on long-term reliability of crystalline silicon photovoltaic modules," *Microelectronics Reliability*, vol. 53, no. 12, pp. 1922–1926, 2013.